the wave-exciting forces and float forces due to motions which are evaluated from special tests on a single float, has demonstrated good agreement with tests on a free model. The predicted phase relation of motions to wave passage is not as satisfactory as predicted amplitude and should be further investigated.

This approach should be especially useful in design development and in the structural load evaluation of multifloat vehicles and other types of marine structures. The simple apparatus developed for the tests proved effective and should be further developed for testing at lower frequencies of oscillation.

References

[1] Handler, E. H., "Tilt and Vertical Float Aircraft for Open Ocean Operations," *Journal of Aircraft*, Vol. 3, No. 6, Nov.-Dec. 1966, pp. 481–489.

[2] Jayne, G., "Military Applications of Stable Ocean Platforms," paper presented at the Association of Senior Engineers, March 1968, Naval Ship Systems Command, Washington, D.C.

[3] "Directory of Marine Drilling Rigs," *Ocean Industry Magazine*, Vol. 4, No. 3, March 1969, pp. 35–49.

[4] Mercier, J. A., "Motions Response of a Related Series of Vertical Float Supported Platforms in Irregular Seas," Rept. S.I.T.-D.L.-70-1334, Feb. 1970, Davidson Lab. Stevens Institute of Technology, Hoboken, N.J.

[5] Barr, R. A. and Martin, M., "Motions of Tilt-Float Vehicles in Waves," TR 237-1, Oct. 1963, Hydronautics Inc., Laurel, Md.

[6] Mercier, J. A., "A Method for Computing Float Platform Motions in Waves," Rept. 1322, Oct. 1968, Davidson Laboratory, Stevens Institute of Technology, Hoboken, N.J.

[7] Breslin, J. P., Savitsky, D., and Tsakonas, S., "Deterministic Evaluation of Motions of Marine Craft in Irregular Seas," *Proceedings of Fifth Symposium on Naval Hydrodynamics*, Office of Naval Research, 1964, pp. 461–505.

[8] "Nomenclature for Treating the Motion of a Submerged Body Through a Fluid," Technical and Research Bulletin 1-5, April 1950, Society of Naval Architects and Marine Engineers, New York.

[9] Havelock, T. H., "Waves Due to a Floating Sphere Making Periodic Heaving Oscillations," *Proceedings of the Royal Society, Ser. A.*, Vol. 231, 1955, pp. 1–7.

[10] Dewey, D. B. and Fisher, R. R., "Inflatable Float Design Study," Final Report 65-193, Sept. 1965, General Dynamics/Convair, San Diego, Calif.

JULY 1970 J. HYDRONAUTICS VOL. 4, NO. 3

Preliminary Design of Hydrofoil Cross Sections as a Function of Cavitation Number, Lift, and Strength

THOMAS G. LANG*
Naval Undersea Research and Development Center, San Diego, Calif.

A set of graphs and equations is developed for quickly determining the minimum-drag form of noncavitating and supercavitating hydrofoils designed for high Reynolds numbers where the boundary layer is fully turbulent. A single classification parameter is derived which simplifies design selection. The results are applicable to the design of propellers, struts, lifting surfaces, and fins for both submerged vehicles and surface craft. It is shown that hydrofoil cross sections can be classified into six basic types of design forms, five of which are cavitating.

Nomenclature†

b = hydrofoil span (L)
c = chordlength of a hydrofoil (L)
C_d = hydrofoil drag coefficient = $D/\rho U^2bc/2$
C_{dc} = cavity drag coefficient
C_{d0} = cavity drag coefficient when $\sigma = 0$
C_f = skin friction drag coefficient
C_L = lift coefficient = $L/\rho U^2bc/2$
C_{L0} = lift coefficient at $\sigma = 0$; $C_{L0} = C_L - 2\sigma$
C_1 = section modulus coefficient = $2I/t^3c$
D = hydrofoil drag (F)
D_c = cavity drag of a hydrofoil (F)
f = design bending stress, including load factor and factor of safety (FL^{-2})
I = area moment of inertia (L^4)
k = designates the amount of camber of a 2-term hydrofoil camber line
K = hydrofoil classification parameter = $(\sigma - C_L/2)/(M')^{1/2} = \sigma_0/(M')^{1/2} = -C_{L0}/2(M')^{1/2}$
l_c = length of a cavity (L)
L = hydrofoil lift (F)
M = applied bending moment about some cross section of a hydrofoil (FL)
M' = M/fc^3
P = freestream pressure (FL^{-2})
P_v = vapor pressure of the fluid (FL^{-2})
P_1 = minimum pressure on a hydrofoil (FL^{-2})
r = characteristic roughness height (L)
r' = r/c
R = Reynolds number = Uc/ν
t = maximum thickness of a hydrofoil (L)
t' = t/c
t_b = hydrofoil base thickness (L)
t_c = maximum thickness of a cavity (L)
U = freestream velocity (LT^{-1})
U_1 = velocity at the minimum pressure point on a hydrofoil (LT^{-1})
x = chordwise distance to a specific point on a hydrofoil from its leading edge (L)
x' = x/c
y = distance from the chordline to a specific point on a hydrofoil surface (L)
y' = y/c
$y'_l(x')$ = local nondimensional lower-surface height above the chordline

Received April 23, 1969; presented as Paper 69-396 at the AIAA 2nd Advanced Marine Vehicles and Propulsion Meeting, Seattle, Wash., May 21–23, 1969; revision received May 5, 1970.

* Head, Advanced Design Staff, Systems Analysis Group.

† Dimensions are in force F, length L, and time T.

$y'_m(x')$ = local nondimensional meanline height above the chordline
$y'_0(x')$ = nondimensional meanline of the NACA uniform pressure ($a = 1.0$) meanline designed for a unit lift coefficient
$y'_u(x')$ = local nondimensional upper surface height above the chordline
y'_{1-5} = nondimensional heights of hydrofoil parameters listed in Table 2
δ = angle of attack used for generating thickness for a supercavitating hydrofoil, rad
ν = kinematic viscosity of the fluid (L^2T^{-1})
ρ = mass density of the fluid ($FL^{-4}T^2$)
σ = cavitation number = $(P - P_v)/(\rho U^2/2)$
σ_{cr} = incipient cavitation number, i.e., value of σ when cavitation is about to begin as σ reduces
σ_0 = represents σ when $C_L = 0$; $\sigma_0 = \sigma - C_L/2$
τ = designates amount of parabolic thickness added to a hydrofoil
— = terms with a bar over them are defined in Eq. (37)

Introduction

THIS paper is an abstract of the section titled "The Design of Hydrofoil Cross Sections" in the author's Ph.D. thesis[1] on engineering design theory. Consequently, any background information and detailed explanations that have been omitted from this paper may be found in Ref. 1.

Hydrofoils are found in a wide variety of commonly encountered situations. They are used as propeller blades on boats, as sailboat keels, ship rudders, submarine and torpedo fins, lifting surfaces of hydrofoil boats, underwater cable fairings, shroud ring stabilizers for missiles, rotor blades for water jet propulsion units, impeller blades in many kinds of pumps, support struts, etc. The many different uses of hydrofoils have resulted in the development of a wide variety of hydrofoil forms. The streamlined fully-wetted hydrofoils are the most commonly encountered type, and have excellent performance characteristics at speeds up to the beginning of cavitation. Cavitation is characterized by the formation of small cavities filled with water vapor which appear and collapse in the low-pressure region of the hydrofoil surface. As cavitation increases, there is a corresponding increase in the number and degree of such undesirable characteristics as noise, drag, surface pitting, reduction in lift, and unsteady performance. Cavitation can be avoided in certain situations by reducing speed, reducing the hydrofoil thickness or lift coefficient, improving the cross-sectional shape, increasing the freestream pressure, or by operating closer to the design angle of attack of the hydrofoil.

If cavitation cannot be avoided, an entirely different type of hydrofoil can be utilized which provides steady performance, but has somewhat more drag than the best fully-wetted hydrofoils, and produces more noise. One form is called a supercavitating hydrofoil which is analyzed by Tulin and Burkart[2] and operates with its upper surface entirely immersed in a cavity and with its lower surface fully wetted. Another form is a cavitating, nonlifting strut which is analyzed by Tulin[3] and which is entirely immersed in a cavity, except for the nose section.

A third type of hydrofoil is called a base-ventilated hydrofoil, various forms of which are described by Lang.[4] Ventilated hydrofoils characteristically operate with a steady cavity of noncondensing gas in contact with the surface. At cavitation numbers greater than zero, this type has lower drag than a cavitating hydrofoil, and it operates more quietly. Its use requires a gas source to maintain the cavity.

For the purpose of this paper, it is assumed that a gas source is not available and that the hydrofoils are either fully wetted or else designed for cavitation. Some of the advantages and disadvantages of the various hydrofoil cross sections will become evident later.

Specification of the Design Problem

Many hydrofoil design problems can be reduced to the need for a hydrofoil cross section which provides a certain lift coefficient, sustains a given bending moment, and operates well at a given cavitation number, Reynolds number, etc. Typical hydrofoil cross sections are sketched in Fig. 1. The objective of this design problem is to determine the hydrofoil cross-sectional forms which have minimum drag. For simplicity, it is assumed that the flow is steady, that the only critical stress is bending stress, that all cross sections are solid, that the water surface is sufficiently far away so that it has no hydrodynamic effect, that no tensile forces exist in the fluid, that cavity walls are smooth, and that the angle of attack is fixed at the design angle.

Design Problem Variables.

The design problem variables are assumed to be the design stress f of the structural material,‡ hydrofoil chordlength c, characteristic surface roughness r, freestream speed U, freestream pressure P, fluid viscosity ν, fluid density ρ, fluid vapor pressure P_v, lift per unit span L/b, and applied bending moment M. In summary, the 10 design problem variables are f, c, r, U, P, ν, ρ, P_v, L/b, and M. Applying the design procedure of Ref. 1, the dimensional variables are reduced to five nondimensional design mission variables. These new variables characterize a nondimensional design problem, and are the lift coefficient C_L, moment coefficient M', cavitation number σ, Reynolds number R, and roughness ratio r' where

$$C_L = (L/b)/c\tfrac{1}{2}\rho U^2 \quad (1)$$

$$M' = M/fc^3 \quad (2)$$

$$\sigma = (P - P_v)/\tfrac{1}{2}\rho U^2 \quad (3)$$

$$R = Uc/\nu \quad (4)$$

$$r' = r/c \quad (5)$$

Optimization Criterion

The objective of the nondimensional design problem is to minimize the drag coefficient C_d, where

$$C_d = (D/b)/c\tfrac{1}{2}\rho U^2 \quad (6)$$

where D/b is the drag per unit span.

Physical Relationships

The relationship for bending stress is considered first. The design bending stress of the minimum-drag hydrofoil cross section must be equal to the actual bending stress, so

$$f = M/C_1(t/c)^2c^3 \quad (7)$$

where t = hydrofoil thickness, and C_1 is the section modulus coefficient. Rearranging,

$$M' = M/fc^3 = C_1(t/c)^2 \quad (8)$$

Cavitation is considered next. Let P_1 be the minimum pressure at some point on a fully-wetted hydrofoil where the local velocity is U_1. According to the Bernoulli equation, P_1 is

$$P_1 = P + \tfrac{1}{2}\rho U^2 - \tfrac{1}{2}\rho U_1^2 = P + \tfrac{1}{2}\rho U^2[1 - (U_1/U)]^2 \quad (9)$$

Cavitation will occur when P_1 reduces to the vapor pressure of the fluid P_v (assuming no tensile stress in the fluid). The critical (incipient) cavitation number is defined as

$$\sigma_{cr} = (P - P_1)/\tfrac{1}{2}\rho U^2 = (U_1/U)^2 - 1 \quad (10)$$

Cavitation will occur whenever $\sigma < \sigma_{cr}$ where σ is the cavitation number.

‡ The design stress includes the load factor and the factor of safety.

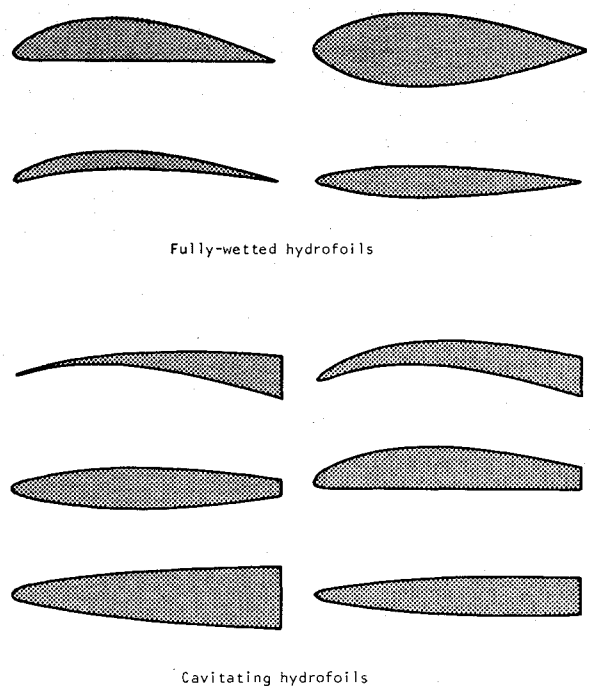

Fig. 1 Typical hydrofoil forms.

It will now be shown that R and r' can be eliminated from the list of important variables. The Reynolds number R determines how the hydrofoil should be formed to best utilize laminar flow, prevent laminar separation, prevent turbulent separation, and minimize skin-friction drag. However, R is not normally critical in the range $R > 10^7$ because the boundary layer is generally fully turbulent, and changes in Reynolds number in this range have only a small effect on hydrofoil form. Also, it is known that the roughness ratio r' has little effect on hydrofoil form if it does not exceed certain critical values which depend upon R; the roughness can generally be kept below these values.

In view of this discussion, it is seen that the nondimensional design problem can be simplified by assuming that $r' = 0$ and $R \gg 10^7$; the results will still be very general and useful. The design variables are consequently reduced to C_L, M', and σ. In order to approach this three-dimensional (i.e., three-variable) design problem, the simpler two-dimensional design problems will be considered first where one of the three variables is assumed to be zero.

Design Problem Where $C_L = 0$

The first two-dimensional design problem is where $C_L = 0$ and where M' and σ are variable. Since $C_L = 0$, all points in the two-dimensional design problem space represented by a graph of σ vs M' will be satisfied by uncambered hydrofoils, called hydrofoil struts. All laminar boundary-layer effects can be disregarded since the boundary layer will be fully turbulent at $R \gg 10^7$. The problem reduces to finding the minimum-drag hydrofoil strut section as a function of σ and M', where the boundary layer is turbulent and C_f is very small in view of the high Reynolds number.

As shown in Ref. 1, if the cavitation number is sufficiently high, an efficient fully-wetted streamlined hydrofoil can be designed to satisfy the strength requirement. However, if the cavitation number is low, the most efficient (i.e., minimum-drag) strut is bluff ended and cavitating. Consequently, the graph of M' vs σ will split into two regions where the upper region is satisfied by fully-wetted struts, and the lower region is satisfied by less-efficient cavitating struts.

Fully-Wetted Region

Assuming that the fully-wetted struts have no boundary-layer separation or pressure drag, the minimum-drag form is shown by Ref. 1 to have an elliptical cross section. The pressure is theoretically approximately uniform on both surfaces from a point near the leading edge to a point near the trailing edge. Since the boundary layer will, in actual practice, separate near the trailing edge, a short cusp-shaped or wedge-shaped trailing edge can be added to the basic ellipse to minimize its drag. For the purpose of this paper, however, it will be assumed that the values of C_L, σ, and M' are based upon the chord length c of the basic elliptical section. Reference 1 shows that the stress relationship [Eq. (8)] for an ellipse becomes

$$(\text{ellipse})t/c = (10.2M^1)^{1/2} \tag{11}$$

also, the cavitation relationship [Eq. (10)] becomes

$$(\text{ellipses})\sigma_{cr} = 2t/c \tag{12}$$

Let region I be the portion of the σ vs M' graph which is best satisfied by fully-wetted hydrofoils, and region II be the portion which is best satisfied by cavitating hydrofoils. The boundary between the two regions is obtained from Eqs. (11) and (12) by letting $\sigma_{cr} = \sigma_0$ which gives

$$\begin{pmatrix}\text{boundary between}\\ \text{regions I and IIa}\end{pmatrix} \sigma_0 = 6.39\ (M')^{1/2} \tag{13}$$

where σ_0 designates the value of σ when C_L is assumed to be zero. Equation (11) gives the ellipse ratio t/c as a function of M' for region I where the form is independent of σ.

The drag coefficient for the region I forms is caused by the skin friction only, and is shown by Ref. (1) to be

$$\begin{pmatrix}\text{region I}\\ C_L = 0\end{pmatrix} C_d = 2C_f[6.39(M')^{1/2} + 1] \tag{14}$$

where C_f is the drag coefficient of a flat plate at the Reynolds number R.

Cavitating Region

The cavitating strut family which corresponds to region II is shown by Ref. 1 to be the family of truncated ellipses where

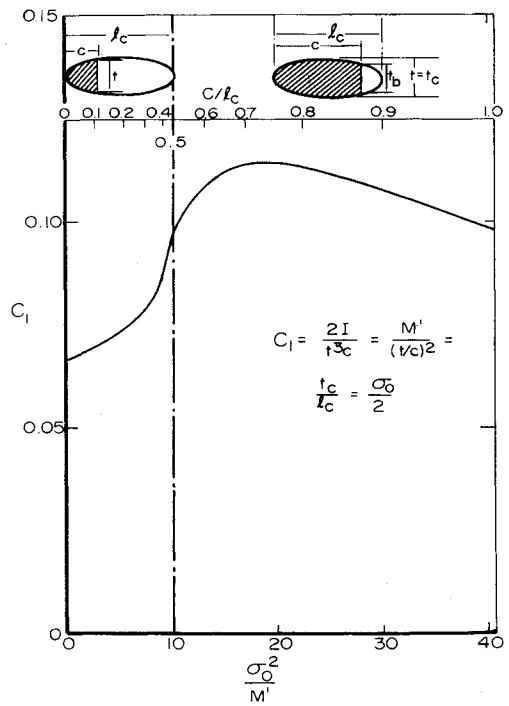

Fig. 2 Section modulus coefficient of truncated elliptical struts.

the strut lies just inside the cavity formed behind its leading edge.

The cavity drag coefficient of a full cavity is shown by Ref. 5 to be

$$C_{dc} = (\pi/8)\sigma_0^2(l_c/c) = D_c/bc\tfrac{1}{2}\rho U^2 \tag{15}$$

where D_c/b is the cavity drag per unit span, and l_c is the cavity length. Assuming that σ_0 is small, Ref. 5 also shows that the shape of a full cavity is an ellipse.

The minimum-drag strut form is a truncated ellipse and is shown by Ref. 1 to be expressed by the following relationships:

$$y' = \begin{cases} \pm\dfrac{\sigma_0}{2}\left[\dfrac{2}{\sigma_0}\left(\dfrac{M'}{C_1}\right)^{1/2}x' - (x')^2\right]^{1/2} \\ \qquad \begin{pmatrix}\text{region IIa} \\ 10.2 \leqq \sigma_0^2/M' \leqq 40.8\end{pmatrix} \\ \pm\dfrac{\sigma_0}{2}\left[\left(\dfrac{M'}{C_1\sigma_0^2}+1\right)x' - (x')^2\right]^{1/2} \\ \qquad \begin{pmatrix}\text{region IIb} \\ 0 \leqq \sigma_0^2/M' \leqq 10.2\end{pmatrix} \end{cases} \tag{16}$$

where y' and x' are the nondimensional semithickness and distance from the leading edge, respectively, and where region IIa corresponds to those struts whose chordlengths are greater than half the cavity length, and region IIb corresponds to those struts whose chordlengths are less than half the cavity length.

Because of the mathematics involved, two different equations are required to define the strut form, and these are called regions IIa and IIb. The equation for the boundary between regions IIa and IIb is seen from the region expressions in Eq. (16) to be

$$\text{(region IIa to IIb boundary)}\quad \sigma_0^2 = 10.2M' \tag{17}$$

The value of the section modulus coefficient C_1 for the two families of truncated ellipses is shown in Fig. 2 as a function of the parameter σ_0^2/M'. This relationship was obtained by 1) integrating over a truncated ellipse to determine the moment of inertia I as a function of c/l_c; 2) calculating the value of C_1 where $C_1 = 2I/t^3c$, and 3) obtaining σ_0^2/M' as a function of c/l_c.

The struts cavitate from their leading edges rearward because their surfaces are designed to lie just inside the cavity in order to eliminate friction drag. Their drag is therefore cavity drag only, and is obtained from Eqs. (15) and (16) as

$$C_d = \begin{cases} (\pi/4)\sigma_0^2(M'/\sigma_0^2C_1)^{1/2}\begin{pmatrix}\text{region IIa} \\ C_L = 0\end{pmatrix} \\ (\pi/8)\sigma_0^2[(M'/\sigma_0^2C_1) + 1]\begin{pmatrix}\text{region IIb} \\ C_L = 0\end{pmatrix} \end{cases} \tag{18}$$

where C_1 is obtained from Fig. 2.

The upper expression in Eq. (18) must be reduced somewhat to include the effect of the thrust produced by impingement of the re-entry jet (which exists at the rear of all cavities) on the strut trailing edge. In view of the lack of experimental data on the re-entry jet effect, it is assumed that half the cavity drag is recovered as thrust when the strut almost fills the cavity, and that the effect tapers to zero recovery when the trailing edge of the cavity is located more than $\frac{1}{4}$ of a cavity length behind the strut.

Table 1 Values of $y'_0(x')$ for the NACA $a = 1.0$ (uniform pressure) meanline at $C_L = 1.0$

x'	0	0.1	0.2	0.3	0.4	0.5
x'	1.0	0.9	0.8	0.7	0.6	0.5
$y'_0(x')$	0	0.0259	0.0398	0.0486	0.0536	0.0552

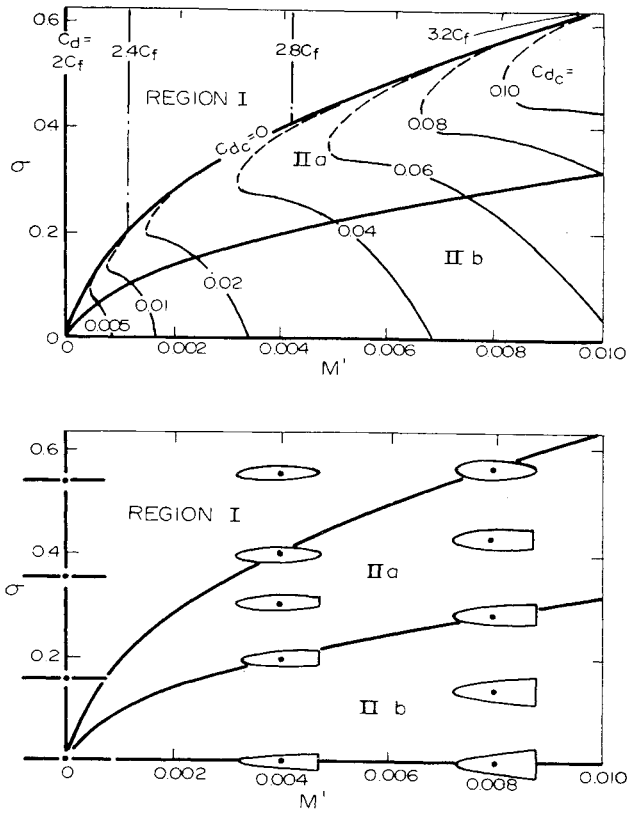

Fig. 3 Hydrofoil struts and drag coefficients for the case when $C_L = 0$.

Illustration of the Design Result

Figure 3 consists of two graphs of σ vs M' which illustrate the design result. Both graphs show the boundaries between regions I, IIa, and IIb. Sketches of the corresponding design forms are superimposed on the lower graph at various selected points. The corresponding value of C_d is plotted on the upper graph of σ vs M'. The dashed lines represent the regions where the re-entry jet influences cavity drag.

Design Problem Where $M' = 0$

This two-dimensional problem is represented by a graph of σ vs C_L, where C_L is selected as the abscissa. Since $M' = 0$, there is no strength requirement, so all forms will have minimum thickness because minimum thickness produces minimum drag. As in the previous design problem, the graph will split into a fully-wetted region I and a cavitating region II.

Region I

Consider first, the noncavitating region where σ is so large that cavitation will not occur. As shown in Ref. 1, all minimum-drag fully-wetted hydrofoils which correspond to this region are cambered meanlines which have a uniform pressure distribution. These cambered lines are the set of NACA $a = 1.0$ meanlines which are presented by Abbot and Doenhoff.[6]

The nondimensional meanline height is expressed as

$$y'_m(x') = y'_0(x')C_L \tag{19}$$

where $y'_0(x')$ is the meanline height for $C_L = 1.0$. Some values for $y'_0(x')$ are reproduced in Table 1 from Ref. 6.

Table 2 Approximate values of $y'_1(x')$ through $y'_5(x')$ for the basic two-term camber, δ-thickness, and parabolic thickness distributions designed for $\sigma = 0$ and infinite depth

x'	0.0	0.05	0.1	0.2	0.4	0.6	0.8	1.0
y'_1	0	0.009	0.017	0.030	0.053	0.073	0.091	0.107
y'_2	0	0.018	0.037	0.071	0.111	0.102	0.038	−0.085
y'_3	0	0.10	0.16	0.25	0.39	0.50	0.59	0.68
y'_4	0	−0.05	−0.10	−0.20	−0.40	−0.60	−0.80	−1.00
y'_5	0	0.22	0.32	0.45	0.63	0.77	0.89	1.00

The drag is assumed to consist solely of turbulent skin-friction drag. Utilizing the velocity distribution as a function of C_L, Ref. 1 shows that the drag coefficient is

$$C_d \doteq 2C_f \tag{20}$$

Also from the velocity distribution, Ref. 1 shows that the critical cavitation number of the region I forms is the boundary expression between regions I and II, which is

$$\text{(regions I and II boundary, } M' = 0) \quad \sigma \doteq \tfrac{1}{2}C_L \tag{21}$$

and which is valid for C_L small relative to 1.0.

Region II

The general form of the cavitating hydrofoil family is shown by Ref. 1 to be a supercavitating profile whose lower surface is fully wetted and whose upper surface is entirely covered by a cavity which springs from the leading edge.

The design of hydrofoil forms for $\sigma = 0$ is considered first. Utilizing the results of Refs. 7–9, the supercavitating forms which have lowest drag when $\sigma = 0$ (for nearly all values of reasonable strength) is described by the parameters k and δ of these references. The parameter k indicates the amount of two-term camber,§ and δ indicates the amount of thickness introduced by angle of attack where

$$k = 0.875C_{L0} \tag{22}$$

$$\delta = 0.0787C_{L0} \tag{23}$$

and where C_{L0} represents C_L when $\sigma = 0$.

The upper and lower coordinates of the hydrofoil surface (assuming that the hydrofoil just fills the cavity) are

$$(\sigma = 0, M' = 0) \begin{cases} y'_u = y'_1(x')k + y'_3(x')\delta \\ y'_l = y'_2(x')k + y'_4(x')\delta \end{cases} \tag{24}$$

where approximate values of $y'_1(x')$ through $y'_4(x')$ are obtained from Ref. 8 and presented in Table 2, together with the values for $y'_5(x')$ which will be utilized later.

The next problem is to determine the best forms for points in region II where $\sigma > 0$. Although both nonlinear and linearized theories exist for determining the lower-surface shape, cavity shape, and lift and drag coefficients for the case when $\sigma > 0$ (Refs. 10–12), the results would require a lengthy computer study to determine which form has the lowest drag for a given C_L, σ, and strength.

A relatively simple solution to this problem is to linearly add the appropriate NACA $a = 1.0$ uniform pressure meanline to the appropriate two-term supercavitating hydrofoil form (and cavity) designed for $\sigma = 0$. The result is a minimum-drag hydrofoil form for $\sigma > 0$. Letting σ be the incipient cavitation number of an NACA $a = 1.0$ meanline, and C_{L0} be the lift coefficient of a two-term hydrofoil form at $\sigma = 0$, the lift coefficient C_L of the linearized combination is approximately

$$\text{(region IIe)} \quad C_L - C_{L0} = 2\sigma \tag{25}$$

where C_L is assumed small; region II is now called region IIe for reasons which will be presented later. Notice that the pressure along the upper surface of the linearized combination, which shall be called the region IIe form, is exactly cavity pressure when $\sigma = \sigma_{cr}$. The nondimensional pressure along the lower surface is approximately the nondimensional pressure at $\sigma = 0$ for the two-term hydrofoil designed for $C_L = C_{L0}$ plus the pressure σ_{cr}. Notice that the NACA $a = 1.0$ meanline is designed for a lift coefficient of $C_L - C_{L0} = 2\sigma$.

The region IIe forms are seen to satisfy the necessary boundary conditions for minimum drag, which are 1) the upper-surface pressure is uniform and matches the cavity pressure, 2) the lower surface is fully wetted, and 3) the resulting form has minimum-thickness and minimum-cavity drag. Furthermore, the region IIe forms are seen to merge into the region I forms at the boundary between regions I and IIe, since $C_{L0} = 0$ along the boundary line where $C_L = 2\sigma$. Therefore, the region IIe forms change smoothly from supercavitating two-term forms designed for $\sigma = 0$ to the NACA $a = 1.0$ meanlines corresponding to the boundary line $\sigma = C_L/2$.

The nondimensional heights of the upper cavity wall and the lower hydrofoil surface y'_u and y'_l, respectively, are

$$\text{(region IIe)} \begin{cases} y'_u = y'_1(x')k + y'_3(x')\delta + y'_0(x')2\sigma \\ y'_l = y'_2(x')k + y'_4(x')\delta + y'_0(x')2\sigma \end{cases} \tag{26}$$

Equation (26) is valid only for low values of C_{L0} because of the assumptions made in the linearized theory; however, Ref. 9 reports negligible error up to $C_{L0} = 0.2$, but that considerable error may exist for $C_{L0} \geqq 0.6$. Therefore, the value of C_L in this analysis is limited to a maximum of 0.6.

The drag coefficient for the region IIe forms is shown by Ref. 1 to be

$$\text{(region IIe)} \quad C_d = 0.142(C_L - 2\sigma)^2 + \frac{0.236\sigma^2(C_L - 2\sigma)}{\sigma + 0.71(C_L - 2\sigma)} + C_f\left(1 - \frac{C_L}{2} + \frac{\sigma}{2}\right)^2 \tag{27}$$

where the last term is friction drag and the other terms are cavity drag.

Illustration of the Design Result

Some of the hydrofoil forms corresponding to the graph of σ vs C_L where $M' = 0$ are shown superimposed on the lower graph of Fig. 4 together with the boundary line between regions I and IIe. The corresponding values of C_d are plotted in the upper graph. Only the cavity drag is plotted in region IIe since C_f is negligible relative to C_{dc} when $R_e \gg 10^7$. Values of C_L are plotted only up to 0.60 because of the limitations of the linearized theory. The most practical range of C_L for supercavitating hydrofoils is around 0.20, so the coverage is adequate.

Design Problem Where $\sigma = 0$

Since $\sigma = 0$, all points in the graph of C_L vs M' will correspond to supercavitating design forms consisting of different combinations of the two-term camber configuration repre-

§ Called "two-term" in view of the number of terms in a certain trigonometric series used in defining the pressure distribution.

sented by k, parabolic thickness represented by τ, and angle-of-attack thickness represented by δ.

Reference 1 shows that region II splits into the following families of supercavitating hydrofoils:

$$\begin{pmatrix}\text{region IIc}\\ \sigma = 0\end{pmatrix} 0.0502C_{L0}^2 \leqq M'$$

$$\text{where } \begin{cases} k = 0 \\ \delta = (2/\pi)C_{L0} \\ \tau = 1.93(M' - 0.0014C_{L0}^2)^{1/2} - 0.426C_{L0} \end{cases} \quad (28)$$

$$\begin{pmatrix}\text{region IId}\\ \sigma = 0\end{pmatrix} 0.0016C_{L0}^2 \leqq M' \leqq 0.0502C_{L0}^2$$

$$\text{where } \begin{cases} \tau = 0 \\ k = 0.962C_{L0} - 4.35(M' - 0.0012C_{L0}^5)^{1/2} \\ \delta = 0.024C_{L0} + 2.76(M' - 0.0012C_{L0}^2)^{1/2} \end{cases} \quad (29)$$

$$\text{(region IIe) } 0 \leqq M' \leqq 0.0016C_{L0}^2 \begin{cases} \tau = 0 \\ k = 0.875C_{L0} \\ \delta = 0.079C_{L0} \end{cases} \quad (30)$$

where C_{L0} is defined as

$$C_{L0} = C_L - 2\sigma \quad (31)$$

The upper- and lower-surface coordinates are

$$\begin{pmatrix}\text{regions IIc,}\\ \text{IId, and IIe}\end{pmatrix} \begin{cases} y'_u = y'_1(x')k + y'_3(x')\delta + y'_5(x')\tau \\ y'_l = y'_2(x')k + y'_4(x')\delta - y'_5(x')\tau \end{cases} \quad (32)$$

where the values of $y'_1(x')$ through $y'_5(x')$ are listed in Table 2.

The drag coefficient for all region II forms when $\sigma = 0$ is shown by Ref. 1 to be

$$\text{(region II, } \sigma = 0) \; C_d = [0.319k + 1.25(\tau + \delta)]^2 + C_f[1 - (C_{L0}/2)]^2 \quad (33)$$

The lower graph of Fig. 5 illustrates the design result where $\sigma = 0$, and M' is plotted against C_L. Sketches of the corresponding design forms are superimposed. The upper graph of Fig. 5 shows the values of the cavity drag coefficient, which is Eq. (33) less the last term.

Solution of the Entire Three-Dimensional Design Problem

The solutions to the three previous two-dimensional design problems can be used as guides in solving the three-dimensional problem represented by the three coordinates, C_L, M', and σ. The same physical equations are used, and the same general design concepts are applied. The expressions for the hydrofoil forms, their drag coefficients, and the boundaries between regions I and IIa–e in the three-dimensional space of C_L vs M' vs σ, will be presented later. The boundaries, as derived in Ref. 1, are shown in Fig. 6, and the corresponding hydrofoil forms are shown superimposed in five different planes of the three-dimensional space in Fig. 7. Notice how the optimum hydrofoil forms change continuously between any two points in the three-dimensional space.

Transformation of the Three-Dimensional Design Problem into a One-Dimensional Design Problem

As a result of solving the three-dimensional design problem, Ref. 1 shows that a significant simplification takes place by introducing the parameter K where

$$K = (\sigma - C_L/2)/(M')^{1/2} \quad (34)$$

Alternatively, K may be expressed as

$$K = \sigma_0/(M')^{1/2} \quad (35)$$

or

$$K = -C_{L0}/2(M')^{1/2} \quad (36)$$

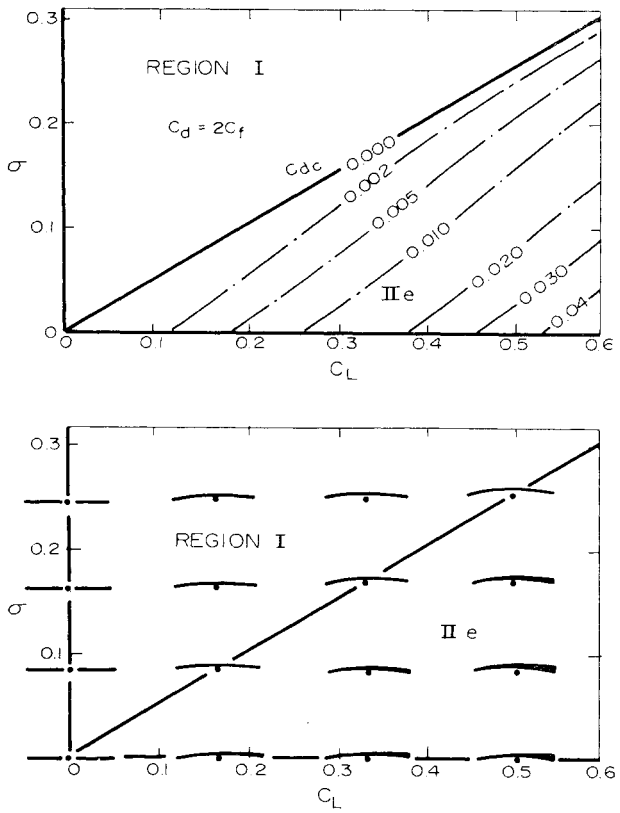

Fig. 4 Hydrofoil forms and drag coefficients for the case when $M' = 0$.

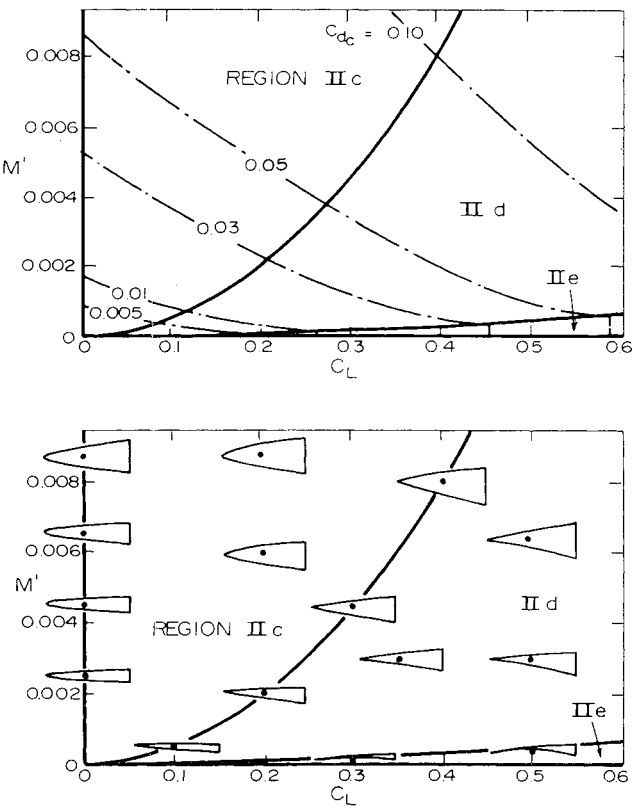

Fig. 5 Hydrofoil forms and drag coefficients for the case when $\sigma = 0$.

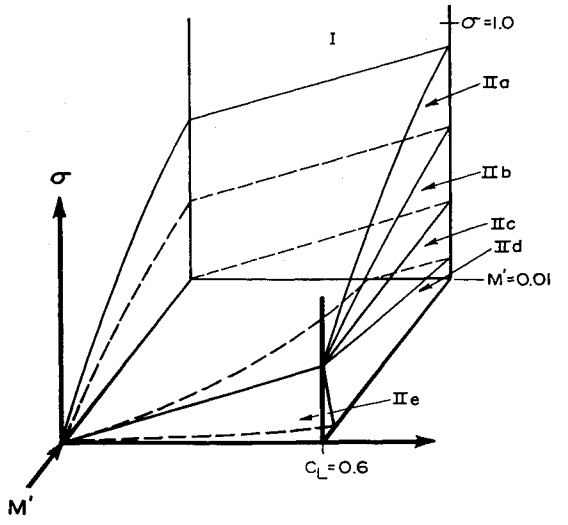

Fig. 6 Boundaries of regions I-IIe in three-dimensional space.

The equations for the region boundaries are expressed solely as a function of K in Table 3.

The simplification introduced for the description of the boundaries can be extended to the description of the hydrofoil forms and the drag coefficients. The following definitions are introduced:

$$\begin{aligned}
\bar{C}_L &= C_L/(M')^{1/2} \\
\bar{\sigma} &= \sigma/(M')^{1/2} \\
\bar{y}' &= y'/(M')^{1/2} = (y/c)/(M')^{1/2} \\
\bar{t}' &= t'/(M')^{1/2} = (t/c)/(M')^{1/2} \\
\bar{\delta} &= \delta/(M')^{1/2} \\
\bar{\tau} &= \tau/(M')^{1/2} \\
\bar{k} &= k/(M')^{1/2} \\
\bar{C}_{dc} &= C_{dc}/M' \\
\bar{C}_{d0} &= C_{d0}/M'
\end{aligned} \tag{37}$$

Table 3 Region boundaries for subspace (f) as a function of K

Region boundary	Equation
I to IIa	$K = 6.39$
IIa to IIb	$K = 3.19$
IIb to IIc	$K = 0$
IIc to IId	$K = -2.23$
IId to IIe	$K = -12.5$

where

$$C_{dc} = C_{d0} + \{(\pi/4)[\sigma(t/c)]^2/[\sigma(t/c) + 1.5C_{d0}]\} \tag{38}$$

Equation (38) is an empirical relationship developed in Ref. 1 from theory presented in Refs. 13 and 14.

The hydrofoil forms as a function of K, C_1, and the new variables defined by Eq. (37) are listed in Table 4. The values for C_1 are shown in Fig. 2 as a function of K^2. The forms and drag coefficients for the truncated ellipses of regions IIa and IIb are presented in Fig. 8. The expressions for C_{d0} and the frictional drag coefficient C_{df} are listed for all hydrofoils in Table 5.

The basic form characteristics which consist of $\bar{t}' = (t/c)/(M')^{1/2}$, t_b/t, $\bar{\tau}$, $\bar{k}/10$, and $\bar{\delta}$ are plotted in Fig. 9 as a function of K. Also shown in Fig. 9 are typical hydrofoil shapes superimposed along vertical lines which represent the region boundaries. Notice how clearly and precisely Fig. 9 presents all of the hydrofoil forms and how the three-dimensional illustration in Fig. 7 has been condensed into a single one-dimensional graph where the only parameter is K. The parameter K classifies all cavitating hydrofoils and the simpler fully-wetted hydrofoils much like the specific speed parameter classifies turbomachinery. The nature of the parameter K is somewhat broader than the specific speed parameter, however, because it includes the effect of cavitation and structural strength on design form which the latter does not. Figure 9 can be utilized together with Tables 4 and 5, Eqs. (37) and (38), and Figs. 2 and 8, to completely specify the lowest-drag hydrofoil cross section as a function of C_L, M', and σ.

Table 4 Hydrofoil form characteristics[a]

Region	Form equation	$\bar{t}' = (t/c)/(M')^{1/2}$	t_b/t
I	$\bar{y}'_u = 3.19[x' - (x')^2]^{1/2} + y'_0\bar{C}_L$ $\bar{y}'_l = -3.19[x' - (x')^2]^{1/2} + y'_0\bar{C}_L$	3.19	0
IIa	$\bar{y}'_u = \frac{K}{2}\left[\frac{2x'}{K(C_1)^{1/2}} - (x')^2\right]^{1/2} + y'_0\bar{C}_L$ $\bar{y}'_l = -\frac{K}{2}\left[\frac{2x'}{K(C_1)^{1/2}} - (x')^2\right]^{1/2} + y'_0\bar{C}_L$	$\frac{1}{(C_1)^{1/2}}$	$K(C_1)^{1/2}\left[\frac{2}{K(C_1)^{1/2}} - 1\right]^{1/2}$
IIb	$\bar{y}'_u = \frac{K}{2}\left[\left(\frac{1}{K^2C_1} + 1\right)x' - (x')^2\right]^{1/2} + y'_0\bar{C}_L$ $\bar{y}'_l = -\frac{K}{2}\left[\left(\frac{1}{K^2C_1} + 1\right)x' - (x')^2\right]^{1/2} + y'_0\bar{C}_L$	$\frac{1}{(C_1)^{1/2}}$	1.0
IIc	$\bar{y}'_u = y'_3\bar{\delta} + y'_5\bar{\tau} + 2y'_0\bar{\sigma}$ $\bar{y}'_l = y'_4\bar{\delta} - y'_5\bar{\tau} + 2y'_0\bar{\sigma}$ $\bar{\delta} = -1.272K$ $\bar{\tau} = 1.93(1 - 0.0056K^2)^{1/2} + 0.85K$ $\bar{k} = 0$	$-0.436K + 3.86(1 - 0.0056K^2)^{1/2}$	1.0
IId	$\bar{y}'_u = y'_1\bar{k} + y'_3\bar{\delta} + 2y'_0\bar{\sigma}$ $\bar{y}'_l = y'_2\bar{k} + y'_4\bar{\delta} + 2y'_0\bar{\sigma}$ $\bar{k} = -1.924K - 4.35(1 - 0.0048K^2)^{1/2}$ $\bar{\delta} = -0.048K + 2.76(1 - 0.0048K^2)^{1/2}$ $\bar{\tau} = 0$	$-0.451K + 3.80(1 - 0.0048K^2)^{1/2}$	1.0
IIe	$\bar{y}'_u = y'_1\bar{k} + y'_3\bar{\delta} + 2y'_0\bar{\sigma}$ $\bar{y}'_l = y'_2\bar{k} + y'_4\bar{\delta} + 2y'_0\bar{\sigma}$ $\bar{k} = -1.750K$ $\bar{\delta} = -0.158K$ $\bar{\tau} = 0$	$-0.602K$	1.0

[a] Note the difference in definition between the lower case k and the capital K symbols.

Table 5 Hydrofoil drag coefficients

Region	$\bar{C}_{d0}$ (or $\bar{C}_{dc}$)	C_{df}
I	0	$2C_f[1 + 6.39(M')^{1/2}]$
IIa	$\bar{C}_{dc} = (\pi/4)\,\sigma/(C_1M')^{1/2}$	$C_f[1 - (C_L/2) + \sigma/2]^2$
IIb	See Fig. 8	...
IIc	$[2.41(1-0.0056K^2)-0.525K]^2$	...
IId	$[2.06(1-0.0048K^2)-0.674K]^2$	...
IIe	$0.572K^2$	...

General Comments on the Design of Hydrofoil Cross Sections

The results of this hydrofoil design problem are applicable to a wide variety of operating situations. The restrictions that $R_e \gg 10^7$ and $r' = 0$ are not necessary as long as the boundary layer is turbulent; an expression for the frictional drag has been included to correct all drag coefficients for R and r'. The turbulent boundary-layer restriction is not necessary for the case of the cavitating region II forms. The design assumption that there is negligible effect of the water surface on performance is often not important, since many hydrofoils do not operate less than two chordlengths of the surface where depth affects become significant. The restriction that $\Delta\alpha = 0$ can be relaxed to $\Delta\alpha = \pm 3°$ for fully-wetted hydrofoils when the boundary layer is turbulent, without seriously influencing the performance or design form, unless cavitation is very critical. The effect of short periods of positive values of $\Delta\alpha$ on supercavitating hydrofoil performance or design form is small; however, if $\Delta\alpha$ is to be negative, the upper surface should be under cut so that the cavity clears it at negative angles of attack. The restriction to solid sections is not serious because the designer can easily modify the specified M' to account for any amount of hollowness by using a ficticiously high value of M'. Similarly, the assumption that the separation drag of the fully-wetted hydrofoils is negligible can be complied with by adding a cusp-shaped or wedge-shaped trailing edge to reduce separation of the turbulent boundary layer.¶ A final comment is that the results of this analysis can also be made to apply to a relatively new kind of hydrofoil form introduced by Hydronautics, Inc., called a supercavitating hydrofoil with an annex.[15] This form is essentially a typical region II hydrofoil form with an unwetted annex extending rearward into the cavity from the trailing edge to increase the bending strength without changing any of the performance characteristics. Such a form can be treated in this analysis by artificially reducing the required value of M' by perhaps 30% or whatever value the designer finds reasonable in view of the anticipated form of the hydrofoil and cavity. When the design of the region II form has been completed, the designer can add the annex and check his earlier estimate of approximate annex size and strength change. By applying these modifications, the selected conditions for this analysis are found to be significantly extended.

Notice that the optimum hydrofoil forms split into six different families in which each family is described by a different set of equations. Although some of the families

¶ The low-drag fully-wetted hydrofoil forms are very close in shape to an ellipse with either a cusp-shaped or a wedge-shaped trailing edge. For example, see the NACA 16-series and 65-series airfoils of Ref. 6. Also, a sharp trailing edge is necessary in order to satisfy the Kutta condition for the case of lifting hydrofoils. Notice that the value of M' reduces when such a trailing edge is added; this reduction in M' can be accounted for by reducing the specified value of chord length about 20%, or whatever value appears reasonable for the specific thickness-to-chord ratio. Notice that the specified value of C_L has to be changed accordingly. This trailing edge addition affects only the region I forms.

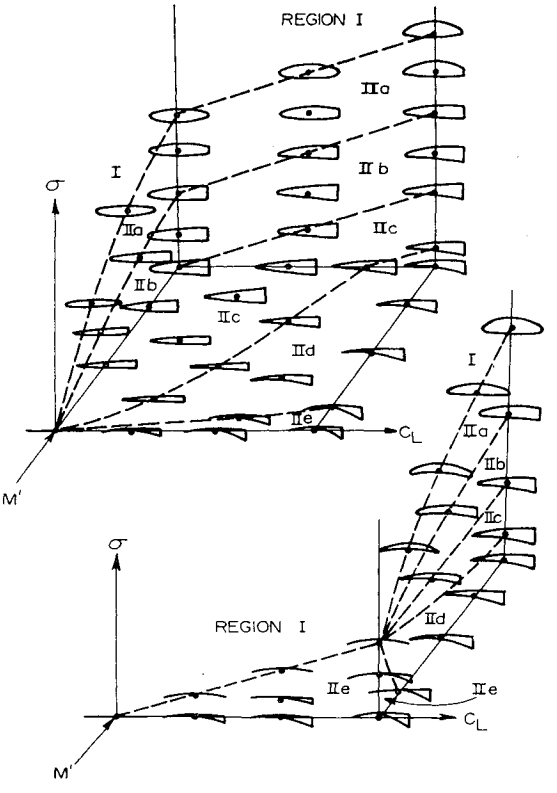

Fig. 7 Illustration of the solution to the three-dimensional design problem.

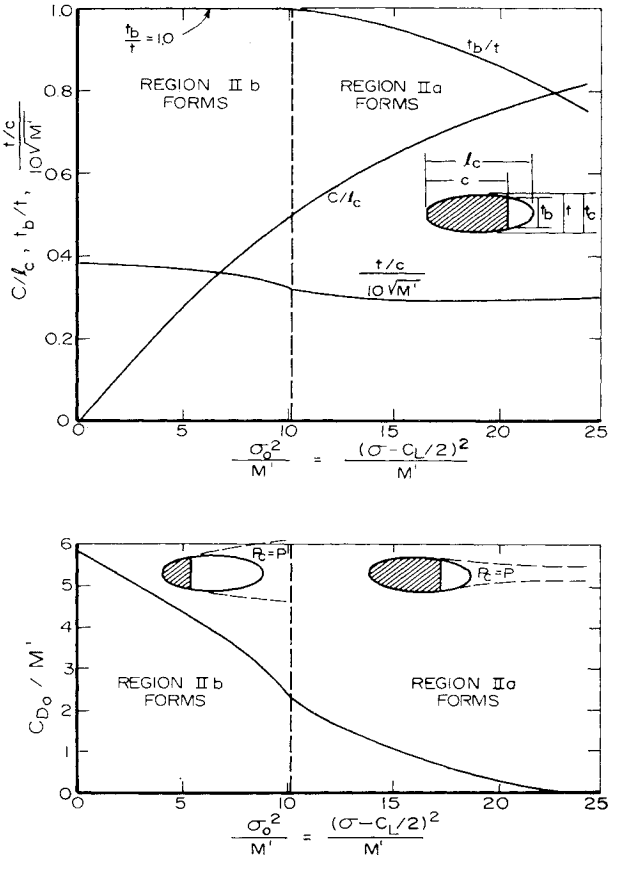

Fig. 8 Drag coefficients and physical properties of truncated ellipses.

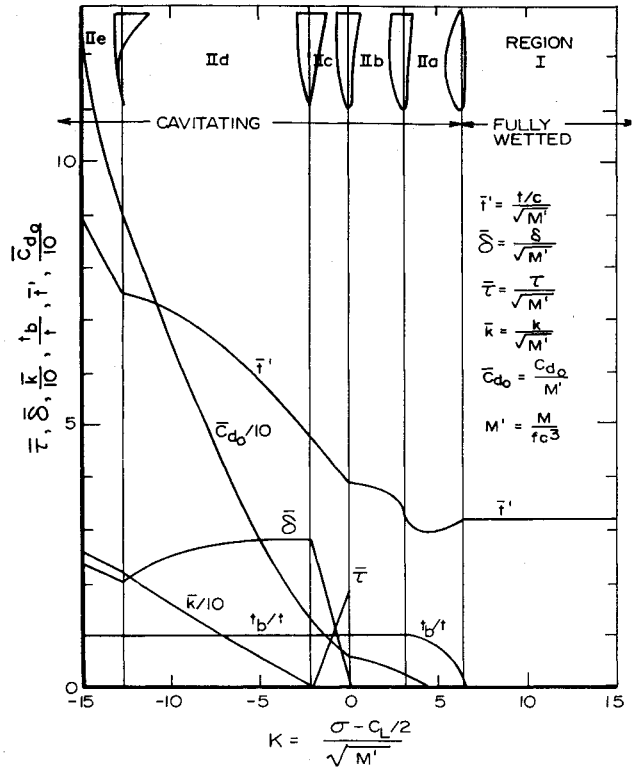

Fig. 9 One-dimensional representation of hydrofoil design form characteristics.

and their boundaries in problem space are uniquely determined, the determination of others is arbitrary and depends upon the variables used in describing the hydrofoil form. For example, the boundary between regions I and II is uniquely determined because it results from a fundamental change in physical flow condition. On the other hand, the boundaries between regions IId–f are not unique because instead of using the variables k, τ, and σ to represent the amount of two-term camber, parabolic thickness distribution, and δ-thickness distribution, other variables could have been used to represent other kinds of basic camber and thickness distributions. Essentially the same hydrofoil form would be found to correspond with each design problem, but the equations describing the forms would be different. Slight form changes and small improvements in performance will probably be found for regions IIc–e as a result of further research into new forms. No changes are anticipated in the forms or boundary description corresponding to regions I, IIa, and IIb within the framework of the stated assumptions. Also, the classification parameter K which resulted from this analysis should remain unique within the framework of the assumptions.

References

[1] Lang, T. G., "A Generalized Engineering Design Procedure," Ph.D. thesis, June 1968, Department of Aerospace Engineering, Pennsylvania State Univ., University Park, P.; also NOWC TP 137, April 1969, Defense Documentation Center.

[2] Tulin, M. P. and Burkart, M. P., "Linearized Theory for Flows About Lifting Foils at Zero Cavitation Number," Rept. C-683, Feb. 1955, The David Taylor Model Basin, Washington, D.C.

[3] Tulin, M. P., "Steady Two-Dimensional Cavity Flows About Slender Bodies," Rept. 834, May 1953, The David Taylor Model Basin, Washington, D.C.

[4] Lang, T. G., "Base-Vented Hydrofoils," NAVORD Rept. 6606, Oct. 1959, U.S. Naval Ordnance Test Station, China Lake, Calif.

[5] Tulin, M. P., "The Shape of Cavities in Supercavitating Flows," TR 121-5, April 1965, Hydronautics Inc., Laurel, Md.

[6] Abbott, I. H. and Von Doenhoff, A. E., *Theory of Wing Sections*, Dover, New York, 1959.

[7] Johnson, V. E., Jr., "Theoretical Determination of Low-Drag Supercavitating Hydrofoils and Their Two-Dimensional Characteristics at Zero Cavitation Number," RML57G11a, Sept. 1957, NACA.

[8] Auslaender, J., "The Linearized Theory for Supercavitating Hydrofoils Operating at High Speeds Near a Free Surface," *Journal of Ship Research*, Oct. 1962, pp. 8–23.

[9] Auslaender, J., "Low Drag Supercavitating Hydrofoil Sections," TR 001-7, April 1962, Hydronautics Inc., Laurel, Md.

[10] Wu, T. Y., "A Free Streamline Theory for Two-Dimensional Fully Cavitating Hydrofoils," *Journal of the Mathematical Physics*, Vol. 35, 1956, pp. 236–265.

[11] Wu, T. Y., "A Note on the Linear and Nonlinear Theories for Fully Cavitated Hydrofoils," Hydro Lab. Rept. 1956, California Institute of Technology, Pasadena, Calif.

[12] Wu, T. Y., "A Wake Model for Free-Streamline Flow Theory; Part I, Fully and Partially Developed Wake Flows and Cavity Flows Past an Oblique Flat Plate," *Journal of Fluid Mechanics*, Vol. 13, 1962, pp. 161–181.

[13] Fabula, A. G., "Application of Thin-Airfoil Theory to Hydrofoils with Cut-Off Ventilated Trailing Edge," NAVWEPS Rept. 7571, Sept. 1960, U.S. Naval Ordnance Test Station, China Lake, Calif.

[14] Fabula, A. G., "Linearized Theory of Vented Hydrofoils," NAVWEPS Rept. 7637, March 1961, U.S. Naval Ordnance Test Station, China Lake, Calif.

[15] Tulin, M. P., "Supercavitating Flows—Small Perturbation Theory," TR 121-3, Sept. 1963, Hydronautics Inc., Laurel, Md.